

trum of the received radiation reveals that apart from the two primary waves numerous satellites appear at frequencies $f_0 \pm n f_2$ and $f_1 \pm n f_2$, where $f_2 = f_0 - f_1$ and n is an integer. This indicates a high degree of remixing of the primary waves with the difference frequency. The physical mechanism may be very similar to that described by Goldman, Davidson, and Hasegawa⁹; they consider the mixing of a high-frequency wave with a low-frequency wave to generate first-order Stokes and anti-Stokes modes. This aspect of the experiment will be dealt with in detail in a forthcoming publication.

Summarizing, we can say that the interaction between unstable waves in a beam-plasma system leads to phenomena that are in general agreement with the theoretical ideas of three-wave coupling in a decay mode. Since the system is nonresonant as far as wave-particle interactions are concerned, the only other nonlinear process that could interfere is particle trapping.¹⁰ The critical trapping field

$$E_{cr} = \frac{1}{4} k \frac{m}{e} (v_{ph} - v_0)^2 = \frac{\sqrt{3}}{32} k \frac{m v_0^2}{e} \left(\frac{\alpha}{\nu_c} \omega_p \right) \quad (5)$$

is of the order of 10 V/cm and well below the fields that may be encountered in the experiment. Although dynamically possible, trapping can nevertheless be ruled out because the transit time of the electrons through the system is smaller than, or at most of the order of, the trapping time $\tau_{tr} = 2\pi(m/ekE)$. An electron can therefore not even execute one oscillation in the potential trough, and the concept of trapping becomes meaningless.

We would like to thank Dr. J. S. Chang and Dr. G. Cooper for making their numerical solutions available.

*Work supported by the Joint Services Electronics Program (U.S. Army, U.S. Navy, and U.S. Air Force) under Contract No. DAAB-07-67-C-0199.

†Present address: 5243 Sandia Laboratories, Albuquerque, N. M. 87115.

‡Permanent address: Department of Physics, Faculty of Science, University of Kyoto, Kyoto, Japan.

¹S. A. Bludman, K. M. Watson, and M. N. Rosenbluth, *Phys. Fluids* **3**, 747 (1960); H. Böhmer, J. Chang, and M. Raether, *Phys. Fluids* **14**, 105 (1971).

²H. Böhmer, J. Chang, and M. Raether, *Plasma Phys.* **11**, 645 (1969).

³P. A. Sturrock, *Phys. Rev. Lett.* **16**, 270 (1966); R. E. Aamodt and M. Sloan, *Phys. Fluids* **11**, 2218 (1968); B. Coppi, M. N. Rosenbluth, and R. N. Sudan, *Ann. Phys. (New York)* **55**, 207 (1969); H. Wilhelmson, L. Stenflo, and F. Engelmann, *J. Math Phys.* **11**, 1738 (1970).

⁴Y. N. Oraevskii and R. Z. Sagdeev, *Zh. Tekh. Fiz.* **32**, 1291 (1962) [*Sov. Phys. Tech. Phys.* **7**, 955 (1963)].

⁵V. N. Tsytovich, *Nonlinear Effects in Plasmas* (Plenum, New York, 1970); R. Z. Sagdeev and A. A. Galeev, *Nonlinear Plasma Theory* (Benjamin, New York, 1969); K. L. Harker and F. W. Crawford, *J. Appl. Phys.* **39**, 5959 (1968).

⁶J. A. Armstrong, N. Bloembergen, J. Ducuing, and P. S. Pershan, *Phys. Rev.* **127**, 1918 (1962).

⁷J. S. Chang and G. Cooper, private communication.

⁸We have calculated W in the collisionless approximation from the second-order dielectric function $\epsilon(2)$. Since there are no resonant particles, Landau damping is negligible and W is real. Starting from the hydrodynamic equations it is a simple matter to include the collision frequency; its influence, however, is very small and can be neglected. Collisions must, however, be retained in the first-order dielectric function for calculating the mode structure.

⁹R. Goldman, R. Davidson, and A. Hasegawa, *Phys. Fluids* **12**, 1247 (1969).

¹⁰W. H. Manheimer, *Phys. Fluids* **14**, 579 (1971); J. R. Thompson, *Phys. Fluids* **14**, 1533 (1971); T. M. O'Neil, J. H. Winfrey, and J. H. Malmberg, *Phys. Fluids* **14**, 1204 (1971).

Nonlocal Instability of Finite-Amplitude Ion Waves

R. A. Stern and J. F. Decker

Bell Telephone Laboratories, Whippany, New Jersey 07981

(Received 20 August 1971)

Instability of electrostatic ion shock waves has been induced by producing an inhomogeneity in the plasma ahead of the wave. A process based on nonlocal instability of precursor ions ejected ahead of finite-amplitude waves is proposed. In addition, instabilities of large-amplitude ion-acoustic waves have been observed and are ascribed to a similar process.

Recent reports have described nonlinear properties of several types of ion waves: ion-acoustic oscillations,¹ shocks,² and solitons.³ The sta-

bility of these waves is a problem of primary and current interest.⁴ We describe here a process which causes turbulent destruction of collision-

less ion shocks and nonlinear ion waves, and which can be attributed to a new physical mechanism—a nonlocal instability excited by precursor ions ejected by the waves. Besides their direct bearing on fundamental properties of waves in plasmas, these observations indicate new processes through which directed energy may become randomized and heat collisionless plasmas.

An essential property of plasma waves are the electric and magnetic fields associated with the waves. These fields interact with charged particles in the plasma, giving rise to phenomena not present in fluids, such as Landau damping and growth. When large-amplitude nonlinear waves steepen into shock or soliton wave fronts,⁵ the finite fields can sweep up some of the charged particles ahead of the wave front, and eject them as a “precursor” charge stream into the unperturbed medium. This streaming can cause Landau growth of ion-acoustic waves ahead of the front if sufficient precursor ions have velocities V_{pr} which resonate with the ion-acoustic-wave phase velocities V_{ia} .⁶ However, for the bulk of precursor ions the ordering of velocities is $V_{pr} > V(\text{wave front}) > V_{ia}$. It follows that processes which can modify the ratio V_{pr}/V_{ia} will determine the stability of the wave-front/precursor system. We point out here that a class of nonlocal processes exists which tends to reduce this ratio to values where strong instabilities can be generated.

A simple example is presented: Consider an inhomogeneous collisionless plasma in which the ions have a position-dependent drift velocity $U(x)$. Ion-acoustic waves propagate at a local speed $\leq (T_e/m_i)^{1/2}$ that is constant relative to the medium, but which has the Doppler-shifted value $V_{ia}(x) \leq (T_e/m_i)^{1/2} + U(x)$ in the laboratory coordinate frame. The precursor ions, however, travel ballistically through the collision-free plasma, maintaining their original space-time trajectories. Therefore when precursor ions move into a plasma where $U(x)$ increases so that the Doppler-shifted $V_{ia}(x)$ increases with position in the direction of precursor motion, a point may be reached when $V_{ia}(x)$ overlaps with V_{pr} , giving rise to instabilities. Similarly, gradients in parameters such as potential or electron temperature, if properly directed, can produce nonlocal instabilities.

Estimates of the inhomogeneity required can be obtained from calculations of ion instabilities.⁷ For an electron-proton plasma with $T_e/T_i = 15$, growth rates as high as 10% of the ion-plasma

frequency are obtained when $V_{pr}/V_{ia} \sim 1.35$. For a weak shock, $M = 1.1$, the precursor peak velocity is $V_{pr \max} = 1.73(T_e/m_i)^{1/2}$ with respect to the medium. Thus a change in the drift velocity of $\sim 0.38(T_e/m_i)^{1/2}$ would suffice to cause instability with an appreciable growth rate, for this typical case.

To observe this effect, shocks were launched into plasmas in which velocity gradients could be generated and controlled. The experiments were carried out in a “double-plasma” device.⁸ This consists of two connecting gas-discharge chambers operated with argon at 10^{-4} Torr, electron density $n_e \sim 10^8 \text{ cm}^{-3}$, and $T_e \sim 1 \text{ eV}$. Ions can be caused to flow into and out of the “target” or observation plasma by applying, respectively, positive and negative voltages to the connecting “driver” plasma. A sufficiently steep positive voltage step causes a shock to develop in the target.⁸ In our scheme, this positive step is preceded by a long-duration negative voltage step which causes (as will be shown quantitatively below) a velocity gradient to form ahead of the shock.

The effect of negative steps on shock structure is illustrated in Fig. 1. In each picture the top trace represents the voltage applied to the driver. The bottom trace shows the electron current drawn by a positively biased, movable Langmuir probe in the target plasma. This current is proportional to the local value of n_e . For small values of the negative voltage, as in trace (a), the density perturbation following application of the positive step exhibits the expected regular shock structure.² The small bump in front of the leading edge of the shock is held to represent precursor ions.^{2,6} As the negative voltage is increased, however, the precursor is found to acquire an oscillatory structure, which tends to engulf the shock. Eventually the shock structure becomes irregular in time, as shown in (b), appearing as a turbulent transition region whose envelope is longer (typically 30 μsec) than the rise time of the excitation pulse (about 15 μsec). Traces (a) and (b) were taken at the same position, 19 cm from the driver; trace (c), a composite, shows the shock at two positions, respectively 4 and 25 cm from the driver. As seen, the shock was initially stable, and acquired its turbulent structure as it progressed across the target plasma. From detailed examination of data, the following conclusions emerge: (i) Starting from conditions which allow development of stable shocks from positive voltage steps, the application of a negative voltage of sufficient amplitude will cause a

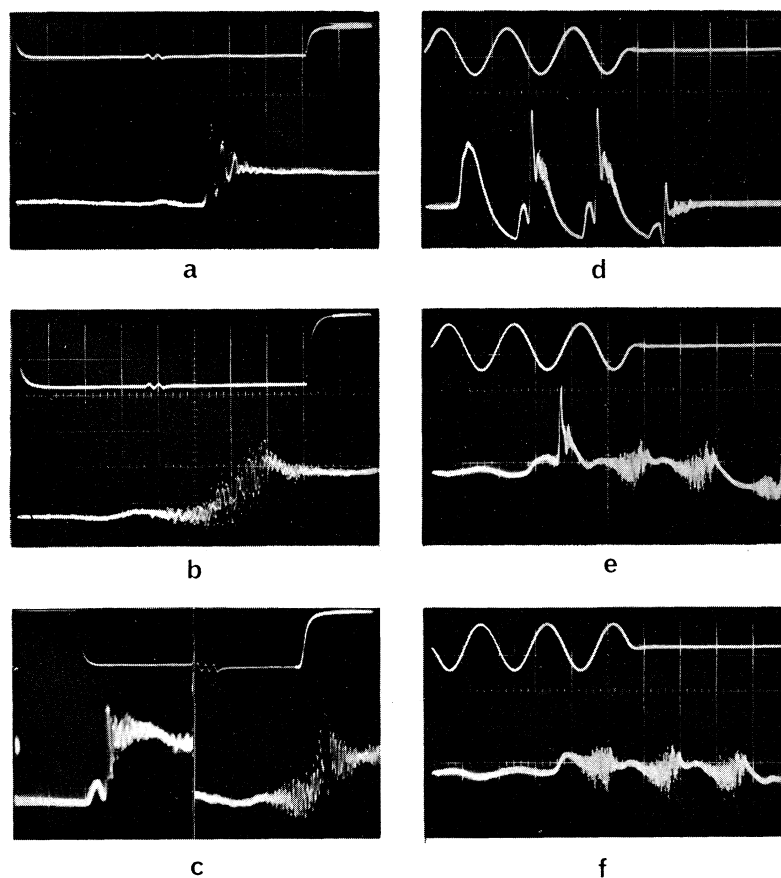


FIG. 1. (a)–(c) Shock turbulence induced by propagation into inhomogeneous plasma. Top traces show voltage applied to driver. Horizontal scale, $100 \mu\text{sec/division}$; vertical scale, 1 V/div . Bottom traces show probe output in target plasma. Horizontal scale, $10 \mu\text{sec/div}$. (a), (b) Effect of increasing negative voltage pulse ahead of shock. Bottom trace, vertical scale 50 mV/div . dc probe output (corresponding to background electron density) $\sim 1.8 \text{ V}$. Probe position 19 cm from driver. (c) Transition to turbulence as function of distance. Bottom vertical scales: left half, 200 mV/div ; right, 50 mV/div . dc probe output $\sim 2.4 \text{ V}$. Positions 4 and 25 cm . (d)–(f) Ion acoustic wave turbulence. Top traces show voltage applied to driver. Horizontal scale, $20 \mu\text{sec/div}$; vertical scale, 2 V/div . Bottom traces show probe output in target chamber. Horizontal scale, $20 \mu\text{sec/div}$. (d), (e) Transition to turbulence as function of distance, first half-cycle positive. (d) Bottom trace, vertical scale 200 mV/div . Probe position, 2 cm . (e) Bottom trace, vertical scale 100 mV/div . Probe position, 12 cm . (f) Effect of starting burst with negative half-cycle. Bottom trace, vertical scale 100 mV/div . dc probe output $\sim 1.65 \text{ V}$. Probe position, 12 cm . Note: Small oscillations in top traces, (a)–(c), indicate test wave used for Fig. 2 (see text).

following shock to become unstable; (ii) the instability develops over a finite propagation distance, and appears first on the precursor; (iii) the shock structure becomes turbulent, random, and the characteristic steepening of applied excitation pulses disappears.

To measure the amplitude of the velocity gradients created in the target plasma by the negative voltage pulses, the space-time trajectories of short oscillatory bursts (ion-acoustic waves) of small amplitude were traced in the target plasma. In Fig. 2, curve (a) corresponds to propagation

in the background plasma (in the absence of a negative voltage). It is a straight-line trajectory, indicative of the uniformity of the background. Its slope, $2.2 \times 10^5 \text{ cm/sec}$, is the linear ion-acoustic wave velocity for an argon plasma with $T_e \cong 1 \text{ eV}$, as expected. Curve (b) shows the same burst when launched $200 \mu\text{sec}$ after a 2-V negative voltage step has been applied. This trajectory is clearly curved. Near the driver (positions $0\text{--}5 \text{ cm}$) the slope yields a propagation velocity (in the laboratory coordinate) which is smaller by 30% than that in the background. Far

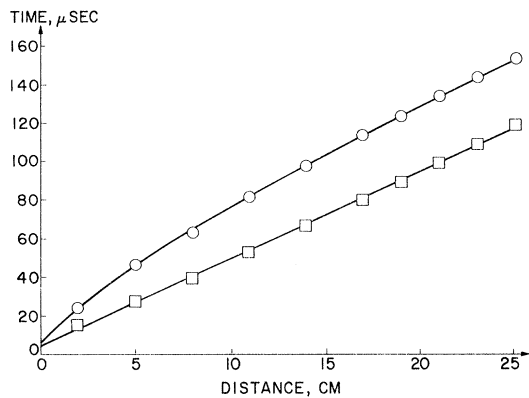


FIG. 2. Space-time trajectory of small-amplitude ion-acoustic burst. Squares, propagation in background plasma; circles, propagation into plasma following application of a 2-V negative voltage to driver. Burst frequency, 25 kHz; peak-to-peak amplitude of probe oscillatory output, 30 mV max; dc probe output, ~ 2.4 V.

from the driver (20–25 cm), the slope becomes asymptotic to the background value. Now the electron temperature can be expected to remain constant throughout the target plasma.⁹ Thus the difference between the wave velocity near the driver and its value at the end of the plasma represent the Doppler shift due to the ion drift-velocity gradient driven by the negative voltage step. This gradient is, as expected, directed towards the driver. A similar shift occurs in the shock propagating into the negative trough. The preceding demonstrates qualitatively that the negative voltage steps which cause shock instability create velocity gradients¹⁰ ahead of the shock, whose direction is precisely that required to reduce the ratio V_{pr}/V_{ia} at points away from the driver and whose amplitude can easily reach values sufficient to cause the nonlocal interaction described above.

We turn now to an extension of this process to ion-acoustic oscillations. Such waves can be viewed as sequences of alternating positive and negative pulses. A positive pulse can steepen and acquire a shock-like structure.¹¹ We note however that a negative pulse, if sufficiently long, should be equivalent in its effect to the negative voltage steps discussed above; i.e., the pulse creates a velocity gradient which could cause a steep wave front to become unstable. To examine this possibility, studies were carried out of the propagation of large-amplitude sine-wave bursts of sufficiently *low frequency*. Figure 1(d) shows an ion-acoustic wave burst, starting with a positive half-cycle, at a position near the driver.

The leading edge of the first positive half-cycle steepens and its trailing edge flattens into a negative ramp. Note however that subsequent positive half-cycles, i.e., those propagating into negative troughs, not only steepen but also acquire a structure and precursor similar to that of the ramp-driven shocks pictured in traces (a) and (c).

Trace (e) shows the same burst, further in the target plasma. The first half-cycle now has acquired the characteristic shock structure, but the following half-cycles exhibit an instability similar to the shocks, as in trace (b). If the burst starts instead with a negative half-cycle, *all* the positive pulses are unstable at this position, as shown in trace (f). From the correspondence between ion-acoustic and shock behavior described here, we conjecture that in ion waves the negative half-cycles can act as local gradients¹⁰ *carried along* with the wave, causing precursor ions ejected by positive half-cycles to become nonlocally unstable. As the wave frequency was increased, the instability disappeared. This contrasts with conventional ion trapping processes, since the latter become more important as the wave frequency increases, i.e., when the wave velocity can approach the ion thermal velocity. Electron trapping would also be more significant at higher frequencies, where the ratio of trapping to collision frequencies increases.⁴

In conclusion, preliminary observations have demonstrated the existence of instabilities of ion shocks and oscillations, associated with their propagation into inhomogeneous plasmas. A non-local process is proposed to explain these observations. Qualitative properties of measured gradients in the plasma are found to be consistent with this model and theoretical estimates. The process is based on the reduction of the ratio V_{pr}/V_{ia} by inhomogeneities in the plasma. It is independent of, and superimposed on, other instability mechanisms such as the reduction in the effective ratio V_{pr}/V_{ia} afforded by two-dimensional effects (resonance between precursor-velocity components and ion-acoustic waves propagating at an angle to the wave front). In addition, it would appear a stabilizing effect could be achieved by reversing the gradient direction in some cases. More general extensions to large-amplitude-wave behavior appear possible and should be considered in evaluating previous results as well as future experiments. Finally, we suggest that energy transfer from directed-wave modes into unstable fluctuations, as demonstrated here, could be of interest for the study of plasma turbulence under

controlled conditions.

It is a pleasure to acknowledge the continual encouragement and many helpful suggestions by N. J. Zabusky, as well as very useful discussions with R. J. Mason and F. D. Tappert.

¹N. Sato, H. Ikezi, Y. Yamashita, and N. Takahashi, *Phys. Rev. Lett.* **20**, 837 (1968), and *Phys. Rev.* **183**, 278 (1969).

²H. K. Anderson, N. D'Angelo, P. Michelsen, and P. Nielsen, *Phys. Rev. Lett.* **19**, 149 (1967), and *Phys. Fluids* **11**, 606 (1968); R. J. Taylor, D. R. Baker, and H. Ikezi, *Phys. Rev. Lett.* **24**, 206 (1970).

³S. G. Alikhanov, V. G. Belan, and R. Z. Sagdeev, *Zh. Eksp. Teor. Fiz., Pis'ma Red.* **7**, 405 (1968) [*JETP Lett.* **7**, 318 (1968)]; H. Ikezi, R. J. Taylor, and D. R. Baker, *Phys. Rev. Lett.* **25**, 11 (1970).

⁴A. V. Gurevich, *Zh. Eksp. Teor. Fiz.* **53**, 953 (1967) [*Sov. Phys. JETP* **26**, 575 (1968)]; K. Nishikawa and C.-S. Wu, *Phys. Rev. Lett.* **23**, 1020 (1969); C. H. Su, *Phys. Fluids* **13**, 1275 (1970); D. W. Forslund and C. R. Shonk, *Phys. Rev. Lett.* **25**, 1699 (1970); R. Z. Sagdeev, in *Reviews of Plasma Physics*, edited by M. A. Leontovich (Consultants Bureau, New York, 1966), Vol. 4 (especially p. 50 ff); D. A. Tidman and N. A. Krall, *Shock Waves in Collisionless Plasmas* (Wiley, New York, 1971) (especially p. 99 ff); S. Abas and S. P.

Gary, *Plasma Phys.* **13**, 262 (1971).

⁵S. S. Moiseev and R. Z. Sagdeev, *J. Nucl. Energy, Part C* **5**, 43 (1963); N. J. Zabusky and M. D. Kruskal, *Phys. Rev. Lett.* **15**, 240 (1965); H. Washimi and T. Taniuti, *ibid.* **17**, 996 (1966); D. Montgomery, *ibid.* **19**, 1465 (1967).

⁶Sagdeev, Ref. 4; Tidman and Krall, Ref. 4.

⁷Abas and Gary, Ref. 4.

⁸R. J. Taylor, H. Ikezi, and K. R. MacKenzie, in *Proceedings of the International Conference on Physics of Quiescent Plasmas* (Ecole Polytechnique, Paris, France, 1969), Pt. 3, p. 57; R. J. Taylor, D. R. Baker, and H. Ikezi, *Phys. Rev. Lett.* **24**, 205 (1970).

⁹For $T_e \sim 1$ eV and a plasma dimension of ~ 25 cm, the transit time for thermally moving electrons across the entire target plasma is about $0.4 \mu\text{sec}$. Therefore, inhomogeneities in the electron temperature in the plasma will be smoothed out in a time very short in comparison with typical periods of plasma waves for our case, specifically $25 \mu\text{sec}$ for a 40-kHz oscillatory burst. This is verified by time-resolved Langmuir probe measurements.

¹⁰Ion rarefaction waves having velocity gradients as described here, and caused by application of a negative voltage to an electrode drawing ion current from a plasma, are discussed by J. E. Allen and J. G. Andrews, *J. Plasma Phys.* **4**, 187 (1970).

¹¹S. G. Alikhanov, R. Z. Sagdeev, and P. Z. Chebotayev, *Zh. Eksp. Teor. Fiz.* **57**, 1565 (1969) [*Sov. Phys. JETP* **30**, 847 (1970)].

Regularization of the Maki Conductivity by Fluctuations*

Joachim Keller† and Victor Korenman

*Department of Physics and Astronomy and the Center for Theoretical Physics,
University of Maryland, College Park, Maryland 20742*

(Received 19 July 1971)

The Maki conductivity for a superconductor above T_c is regularized by taking account of fluctuation effects in the impurity vertex correction.

In a microscopic calculation of the contribution of superconducting pair fluctuations to the dc electrical conductivity of a superconductor above T_c , two terms give the critical temperature dependence. The first, computed by Aslamazov and Larkin¹ (AL), is for a thin film

$$\sigma_{AL}' = e^2/16dt, \quad (1)$$

where d is the film thickness and t the reduced temperature, $t = \ln(T/T_c) \approx (T - T_c)/T_c$. We have set $k_B = \hbar = 1$. Extensive experiments² on highly disordered films of Bi, Pd, and Ga show excellent numerical agreement with this term alone. The second term, calculated by Maki,³ is infinite at all temperatures for one- and two-dimensional

samples. Experimental results on aluminum films⁴⁻⁶ deviate strongly from Eq. (1) and have been fitted, following Thompson,⁷ by including the Maki conductivity, made finite by the assumed presence of a pair-breaking interaction. The Maki-Thompson conductivity is

$$\sigma_{MT}' = (e^2/8d) \ln(t/\delta)(t - \delta)^{-1}, \quad (2)$$

where δ is the pair-breaking strength. By fitting the sum of Eqs. (1) and (2) to a variety of films, δ for aluminum has been found to have the empirical value $\delta = 5 \times 10^{-4} R_{\square}$, proportional to the normal resistance per square of the film, measured in ohms. The origin of the pair breaking has been ascribed to proximity effects, paramagnetic

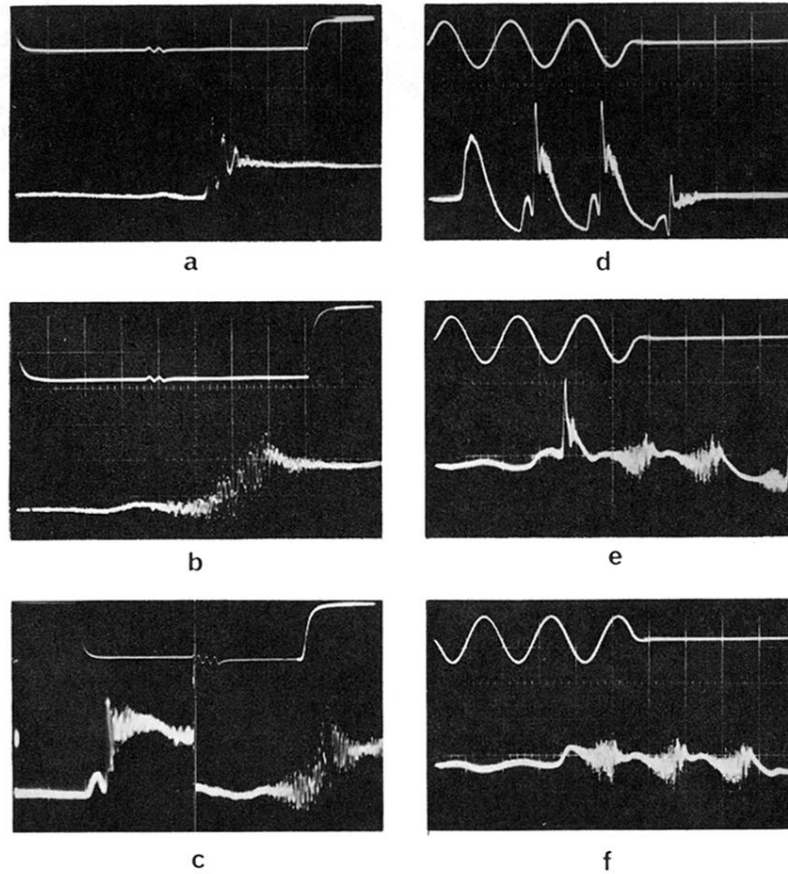


FIG. 1. (a)–(c) Shock turbulence induced by propagation into inhomogeneous plasma. Top traces show voltage applied to driver. Horizontal scale, $100 \mu\text{sec/division}$; vertical scale, 1 V/div . Bottom traces show probe output in target plasma. Horizontal scale, $10 \mu\text{sec/div}$. (a), (b) Effect of increasing negative voltage pulse ahead of shock. Bottom trace, vertical scale 50 mV/div . dc probe output (corresponding to background electron density) $\sim 1.8 \text{ V}$. Probe position 19 cm from driver. (c) Transition to turbulence as function of distance. Bottom vertical scales: left half, 200 mV/div ; right, 50 mV/div . dc probe output $\sim 2.4 \text{ V}$. Positions 4 and 25 cm . (d)–(f) Ion acoustic wave turbulence. Top traces show voltage applied to driver. Horizontal scale, $20 \mu\text{sec/div}$; vertical scale, 2 V/div . Bottom traces show probe output in target chamber. Horizontal scale, $20 \mu\text{sec/div}$. (d), (e) Transition to turbulence as function of distance, first half-cycle positive. (d) Bottom trace, vertical scale 200 mV/div . Probe position, 2 cm . (e) Bottom trace, vertical scale 100 mV/div . Probe position, 12 cm . (f) Effect of starting burst with negative half-cycle. Bottom trace, vertical scale 100 mV/div . dc probe output $\sim 1.65 \text{ V}$. Probe position, 12 cm . Note: Small oscillations in top traces, (a)–(c), indicate test wave used for Fig. 2 (see text).